A wavelet-collocation approach for computational electromagnetics*

Gang Bao[1], G. W. Wei[1,2], and Shan Zhao[1]

[1]Department of Mathematics, Michigan State University, East Lansing, MI 48824, USA
[2]Department of Electrical and Computer Engineering, Michigan State University, East Lansing, MI 48824, USA

Abstract

A wavelet-collocation scheme, constructed from the discrete singular convolution (DSC) is introduced for computational electromagnetics. The basic philosophy behind the DSC algorithm is studied. Four test problems, including waveguide analysis in both regular and irregular domains, electromagnetic wave scattering, electrostatic field estimation via potential functions, and electromagnetic wave propagation in three spatial dimensions, are employed to illustrate the usefulness, test the accuracy and explore the limitation of the wavelet algorithm. Computational accuracy of the wavelet algorithm is shown to be controllable and is compared with a standard approach. Numerical experiments indicate that the proposed wavelet algorithm is a promising approach for solving problems in electromagnetics.

KEYWORDS: Maxwell's equations, waveguide, wave scattering, potential function, wave propagation, wavelet-collocation, discrete singular convolution.

1 Introduction

Recently, computational electromagnetics (CEM) has emerged as a distinct scientific discipline for the study and understanding of a wide variety of electrical and electronic engineering problems[1, 2, 3, 4, 5, 6, 7, 8]. As a natural extension to the analytical approach, the CEM is based on numerically solving the governing equations either in the partial differential form or in the integral equation form. The complexities of physics and of the field geometry are no longer the limiting factors to CEM as they are to the analytical approach. With the advent of high-performance digital computers, CEM is emerging as a powerful approach for solving practical problems in electromagnetics [1, 2]. As a computational discipline, the success of the CEM is vitally dependent on the virtues of computational algorithms, such as numerical accuracy, stability and efficiency. These in turn depend on grid methods and numerical schemes for the solution of the Maxwell's equations.

Typically, grid methods used in CEM are either local, such as finite difference (FD) methods [2], or global, such as Fourier pseudospectral methods [3]. Global methods are highly accurate but are cumbersome to implement in complex geometries and non-conventional boundary conditions. In contrast, local methods are easy to implement for complex geometries and discontinuous boundary conditions. However, the accuracy of local methods is relatively low[4]. There exists

*Email addresses: bao@math.msu.edu (Gang Bao), wei@math.msu.edu (G. W. Wei), szhao@math.msu.edu (Shan Zhao)

Report Documentation Page

Form Approved
OMB No. 0704-0188

1. REPORT DATE	2. REPORT TYPE	3. DATES COVERED
23 APR 2004	**N/A**	**-**

4. TITLE AND SUBTITLE	5a. CONTRACT NUMBER
Awavelet-collocation approach for computational electromagnetics	5b. GRANT NUMBER
	5c. PROGRAM ELEMENT NUMBER
6. AUTHOR(S)	5d. PROJECT NUMBER
	5e. TASK NUMBER
	5f. WORK UNIT NUMBER
7. PERFORMING ORGANIZATION NAME(S) AND ADDRESS(ES) **Department of Mathematics, Michigan State University, EastLansing, MI 48824,USA**	8. PERFORMING ORGANIZATION REPORT NUMBER
9. SPONSORING/MONITORING AGENCY NAME(S) AND ADDRESS(ES)	10. SPONSOR/MONITOR'S ACRONYM(S)
	11. SPONSOR/MONITOR'S REPORT NUMBER(S)

12. DISTRIBUTION/AVAILABILITY STATEMENT
Approved for public release, distribution unlimited

13. SUPPLEMENTARY NOTES
See also ADM001763, Annual Review of Progress in Applied Computational Electromagnetics (20th) Held in Syracuse, NY on 19-23 April 2004.

14. ABSTRACT

15. SUBJECT TERMS

16. SECURITY CLASSIFICATION OF:			17. LIMITATION OF ABSTRACT	18. NUMBER OF PAGES	19a. NAME OF RESPONSIBLE PERSON
a. REPORT	b. ABSTRACT	c. THIS PAGE			
unclassified	**unclassified**	**unclassified**	**UU**	**8**	

many problems in CEM which require both high computational accuracy and high numerical flexibility in handling complex geometries. These problems are characterized by a geometry which has a large domain size, i.e., the dimensions of the scatterer greatly exceed the wavelength of the incident wave. A typical example is the radar cross-section analysis of an entire airplane with an incident electromagnetic wave having a frequency of the order of ten GHz. To deal with such problems, it is desired to have a computational method that has both global methods' accuracy and local methods' flexibility.

Wavelet-based algorithms are expected to fill this gap, and wavelet analysis has been applied to CEM [7, 8]. More recently, the discrete singular convolution (DSC) algorithm was proposed as a potential wavelet approach for the computer realization of singular convolutions[9]. The mathematical foundation of the algorithm is the theory of distributions and the theory of wavelets [10, 11]. By appropriately selecting parameters of a DSC-wavelet kernel, the DSC-wavelet approach exhibits controllable accuracy for integration and shows great flexibility in handling complex geometries and boundary conditions. It was demonstrated that in the framework of the DSC algorithm, different numerical schemes, such as global, local, Galerkin, collocation, and FD, can be deduced from a single starting point[12].

The purpose of this paper is to introduce the DSC-wavelet algorithm for CEM. The potential of the wavelet algorithm for CEM is explored through applications to waveguide analysis, wave scattering, electrostatics analysis, and wave propagation.

2 The Discrete Singular Convolution and wavelets

In the DSC-wavelet algorithm, it is convenient to formulate the numerical solution in terms of the collocation scheme for solving PDEs [12]. For the collocation scheme, an approximation to the derivatives is required given that function values $\{f(x_m)\}$ at a set of discrete points $\{x_m\}$ are known. In the DSC algorithm, we approximate the function and its nth order derivative at point x by a discrete convolution

$$f^{(n)}(x) \approx \sum_{k=-M}^{M} \delta_{\alpha,\sigma}^{(n)}(x - x_k) f(x_k) \qquad (n = 0, 1, 2, \cdots), \tag{1}$$

where $2M + 1$ is the computational bandwidth and $\{x_k\}$ are centred around x. Here $\delta_{\alpha,\sigma}(x - x_k)$ is a collective symbol for one of the (regularized) DSC kernels, or in general, any delta sequence kernel which provides an approximation to the delta distribution δ [9]. For a given $\delta_{\alpha,\sigma}(x - x_k)$, the higher order derivative terms can be given by means of *analytical* differentiation $\delta_{\alpha,\Delta}^{(n)}(x-x_k) = \left[\left(\frac{d}{dx}\right)^n \delta_{\alpha,\sigma}(x - x_k)\right]$. Numerical solution of differential equations then can be easily implemented in a collocation scheme by using Eq. (1). Moreover, the wavelet collocation has been shown to be equivalent to a wavelet Galerkin [12].

In the DSC algorithm, delta sequence kernels can be constructed as either positive type or Dirichlet type [11]. The Dirichlet type kernels are well-suited to be utilized in a wavelet-collocation approach, while the positive type kernels can be used in a wavelet-Galerkin scheme. A family wavelet delta kernels including both types have been constructed [9]. For simplicity, only a few relevant delta sequence kernels of Dirichlet type are considered here, i.e., Dirichlet kernel, Lagrange kernel, and Shannon kernel. The Shannon kernel is the well known scaling function for Shannon

wavelets, which play a crucial role in information theory and the theory of signal processing. However the usefulness of Shannon delta kernel for solving PDE is limited by the fact that it is non-local.

In the DSC-wavelet algorithm, a regularization procedure is typically applied to improve the smoothness, regularity and localization of a temper distribution by using the Gaussian [9]. In this manner, we construct the following three DSC-wavelet kernels, i.e., a regularized Shannon's kernel (RSK), a regularized Dirichlet kernel (RDK), and a regularized Lagrange kernel (RLK) [9], where Δ is the grid spacing,

$$\delta_{\Delta,\sigma}(x-x_k) = \frac{\sin\frac{\pi}{\Delta}(x-x_k)}{\frac{\pi}{\Delta}(x-x_k)} \exp\left[-\frac{(x-x_k)^2}{2\sigma^2}\right], \tag{2}$$

$$\delta_{\Delta,\sigma}(x-x_k) = \frac{\sin\left[\frac{\pi}{\Delta}(x-x_k)\right]}{(2L+1)\sin\left[\frac{\pi}{\Delta}\frac{x-x_k}{2L+1}\right]} \exp\left[-\frac{(x-x_k)^2}{2\sigma^2}\right], \tag{3}$$

$$\delta_{\Delta,\sigma}(x-x_k) = \prod_{i=k-L,i\neq k}^{i=k+L} \frac{x-x_i}{x_k-x_i} \exp\left[-\frac{(x-x_k)^2}{2\sigma^2}\right]. \tag{4}$$

3 Numerical experiments

In this section, we explore the utility of the wavelet-collocation approach for solving problems in electromagnetics. Four different CEM problems are considered. In the wavelet algorithm, the half bandwidth, M, is set to 40 in all calculations except where specified. In the regularized Dirichlet and Lagrange kernels, (3) and (4), L is set to 50 in calculations. The wavelet parameter $r = \sigma/\Delta$ is optimized for each M and reported. The standard second-order central FD method is also considered for a comparison.

3.1 Waveguide analysis

EIGENMODE ANALYSIS We first consider the problem of finding waveguide eigen-modes. Consider a rectangular waveguide, with propagation in the z-direction. For the transverse magnetic (TM) mode, the E_z field component can be expressed as $E_z(x,y,z,t) = E(x,y)e^{i(\omega t-\alpha z)}$, where E satisfies the Helmholtz equation

$$\frac{\partial^2 E}{\partial x^2} + \frac{\partial^2 E}{\partial y^2} + k^2 E = 0, \tag{5}$$

and vanishes on the boundary ($E = 0$) for the TM modes. The eigenvalue k^2 determines the phase parameter α through $k^2 = \omega^2\mu\epsilon - \alpha^2$, where ϵ and μ are dielectric constant and magnetic permeability, respectively.

In numerical computation, different grid size N is considered for a computational domain, $[0, 10\pi] \times [0, 10\pi]$, and the anti-symmetric boundary extension scheme is employed for the PEC boundaries [9]. By considering both the wavelet and FD methods, the numerical results are listed in Table 1. Here for three DSC-wavelet kernels, we choose $M = N$. When bandwidths are $M = 36, 24$ and 12, the values of $r = \sigma/\Delta$ are chosen as 4.2, 3.2 and 2.65 for the RSK and RDK and 2.95, 2.75 and 2.3 for the RLK. It is obvious in Table 1 that three DSC-wavelet schemes are significantly more accurate than the FD method, especially when representing high-order

Table 1: Absolute errors for waveguide eigenmode analysis. Here 1.7(-2) denotes 1.7×10^{-2}.

N	Scheme	Eigenmode					
		No. 10	No. 20	No. 40	No. 60	No. 80	No. 100
12	FD	1.7(-2)	6.5(-2)	2.5(-1)	3.9(-1)	6.4(-1)	8.6(-1)
	RSK	8.4(-8)	5.2(-7)	1.1(-1)	1.9(-1)	3.2(-1)	4.2(-1)
	RDK	8.8(-8)	5.1(-7)	1.1(-1)	1.9(-1)	3.2(-1)	4.2(-1)
	RLK	2.1(-7)	4.7(-7)	1.1(-1)	1.9(-1)	3.2(-1)	4.2(-1)
24	FD	4.0(-3)	7.9(-3)	2.9(-2)	5.6(-2)	1.5(-1)	3.0(-1)
	RSK	1.8(-14)	9.5(-15)	8.7(-13)	1.4(-8)	8.0(-8)	6.4(-9)
	RDK	3.1(-15)	1.6(-14)	8.5(-13)	1.3(-8)	7.8(-8)	6.3(-9)
	RLK	9.7(-13)	3.2(-12)	5.1(-13)	3.5(-10)	6.3(-9)	3.6(-10)
36	FD	1.7(-3)	3.4(-3)	1.3(-2)	2.5(-2)	6.7(-2)	1.3(-1)
	RSK	1.2(-14)	4.3(-14)	2.2(-16)	7.4(-14)	2.2(-14)	3.7(-14)
	RDK	2.1(-14)	2.1(-14)	3.9(-14)	2.0(-14)	4.2(-14)	1.8(-15)
	RLK	2.9(-14)	1.2(-15)	5.0(-15)	3.8(-14)	6.7(-15)	3.3(-14)

eigenmodes. Furthermore, we note that the RSK and RDK have almost identical performance in all computations. Hence, we only need to consider one of them in the rest of the computation. The performance of the RLK differs slightly from that of the RSK. However, such differences are extremely small. Thus, one can argue that each wavelet kernel performs equally well. This finding is in consistent with those in [9, 12].

For $N = 12$, there are only a maximum of 2.4 grid points per wavelength (PPW) in each dimension. Obviously, if this is the case, it is impossible for any numerical method to exactly catch up with the fast oscillations in high-order eigenmodes. However, under such a low grid density, the DSC-wavelet results are still much better than those of the FD. All three wavelet kernels deliver excellent results when the mesh is refined to 24^2 (about 4.8 PPW in each dimension). Moreover, machine precision is attained for the first 100 eigenmodes when the mesh is further refined to 36^2. However, the accuracy improvement of the FD scheme is negligible and the final results for high-order eigenmodes remain inaccurate.

FIELD DISTRIBUTION In practical applications, the geometry of a waveguide can be very complex so as to achieve certain required properties. Therefore, it is important for a computational algorithm to be flexible enough in handling complex structures. To test the wavelet algorithm in this regard, we consider a specially designed waveguide with its geometry having a T-shape. We are interested in the field distribution of TM (and/or TE) modes of the waveguide. By using the RSK with $r = 4.8$, the obtained field distributions across the cross section for eigenmodes 1, 2, 3 and 4 are shown in FIG. 1(a). Due to complexity in geometry, these eigenmodes are quite localized and do not give the full shape of waveguide confining geometry. However, as plotted in FIG. 1(a), higher-order eigenmodes, 17, 18, 19 and 20, clearly reflect the waveguide geometry. The confining geometry of the waveguide can be seen from mode patterns.

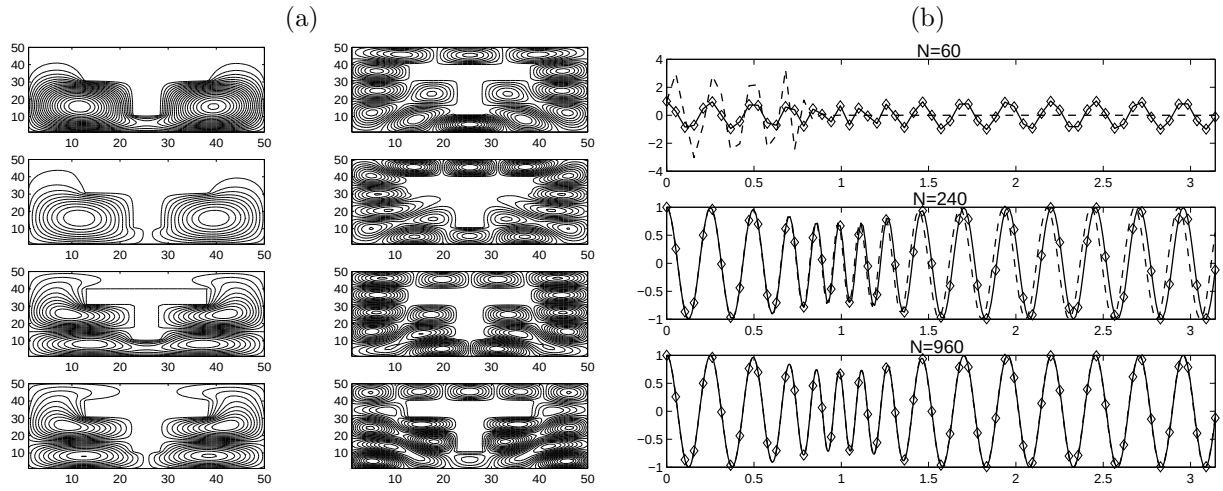

Figure 1: Plots of eigenmodes and scattering fields. (a) Eigenvectors of the T-shape waveguide obtained by using the RSK and a mesh size of 50×50. In (a), left: eigenmodes 1, 2, 3 and 4; right: eigenmodes 17, 18, 19 and 20. (b) Plots of the real part of the scattering wave u. Diamonds: the exact solution; solid lines: the DSC results; and dashed lines: the FD results.

3.2 Wave scattering

Classical problems of wave scattering are usually modeled through an exterior problems governed by the Helmholtz equation with the Sommerfeld radiation conditions imposed at infinity [5]. For the numerical solution of such an exterior problem, an artificial boundary is frequently introduced [5]. In 1D, the resulting model problem over a finite region can be given as [6]

$$u'' + k^2 n^2(x) u = 0, \quad \text{in } [0, \pi], \tag{6}$$

with $u(0) = 1$ and $u'(\pi) - iku(\pi) = 0$. Here k is the wavenumber and $n(x)$ is the index of refraction.

By choosing $k = 25$ and $n(x) = \exp[-10(x-1)^2] + 1$ [6], both the RSK and FD schemes are employed to solve the boundary value problem (6). In the RSK, r is also chosen as 4.8. By using $N = 60$, 240, and 960, the real parts of the simulated waves are plotted in FIG. 1(b). In order to benchmark the numerical results, an exact solution is also shown in FIG. 1(b) which is actually an accurate approximation obtained by using the FD scheme with 3840 points. In terms of the minimal wavelength, the grid density of this problem is 2.4, 9.6, and 38.5 PPW for $N = 60$, 240, and 960, respectively. Since about 18 PPW is required for the FD scheme for accurate modeling [4], the FD results are graphically accurate only when $N = 960$. Amazingly, the wavelet approximation is indistinguishable from the exact solution even when the grid density is as low as 2.4 PPW. Such a under sampling problem remains challenging to other local methods, while the mixed boundary condition may limit the applicability of global methods.

3.3 Electrostatics analysis

In many electromagnetic applications, potential function provides a useful and convenient alternative representation of electromagnetic fields. For electrostatic problems, formulation with the

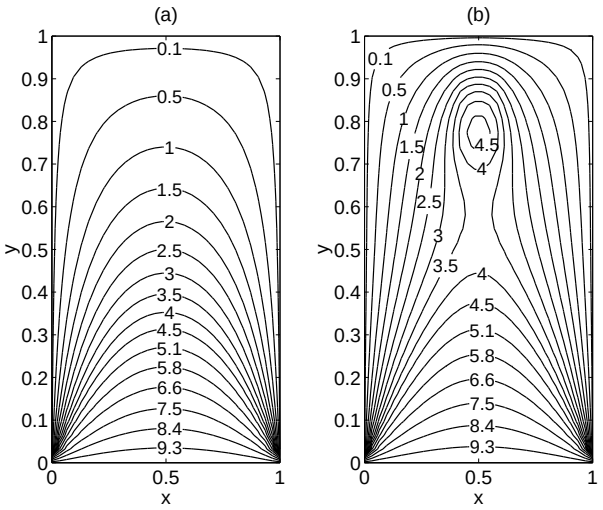

Figure 2: Contour plots of the electric scale potential V. (a) Without charge density; (b) with an area of charge density.

electric scalar potential is known to be the most efficient way to attain the solutions [1]. By representing the electric field $\mathbf{E}$ as the gradient of a scalar potential $\mathbf{E} = -\nabla V$, on attains the electrostatic equation [1]

$$\nabla^2 V = -\frac{\rho}{\epsilon}, \tag{7}$$

where ρ is the volume electric charge density.

To demonstrate the wavelet algorithm for electrostatic calculations, we first consider a simple problem without charge density ($\rho = 0$). The geometry of the problem consists of a conducting square box of $1m \times 1m$ in the $x - y$ plane. The box is infinitely long in the z-direction and thus, this can be regarded as a two-dimensional problem. The potential at the bottom side is considered to be isolated from all other sides with values $V(x, 0) = 10V$ and $V(0, y) = V(1, y) = V(x, 1) = 0$. By choosing 32 points ($N = 32$) in each dimension, the Laplace equation (7) for scale potential function can be directly solved by using the DSC algorithm with $M = 32$ and $r = 3.8$. The anti-symmetric extension is used for all boundaries. The results are plotted in FIG. 2a. We next introduce charge density in the above problem, while the domain and boundary conditions are kept the same. Inside the box, an area of charge density is located at $x : 0.41m - 0.59m,\ y : 0.72m - 0.88m$. The charge density is uniformly distributed within a material of relative permittivity $\varepsilon_r = 25$ and has a value of $\rho = 1.0 \times 10^{-7}[C/m^2]$. Similar to the first problem, the DSC-wavelet approximations of this inhomogeneous problem can be easily generated, see FIG. 2b.

3.4 Electromagnetic wave propagation

In an uncharged homogeneous media, propagation of electromagnetic waves is governed by the wave equation

$$\frac{\partial^2 W}{\partial t^2} - \frac{1}{\epsilon\mu}\nabla^2 W = 0, \tag{8}$$

Table 2: Maximum errors for solving the 3D wave equation.

N	Scheme	M	Δt	$t=4$	$t=10$	$t=16$	$t=22$
24	FD	—	0.2	5.1(-1)	1.2(+0)	1.7(+0)	2.0(+0)
	RSK	6	0.5	1.1(-3)	2.3(-3)	3.5(-3)	4.8(-3)
		12	0.2	2.8(-5)	6.1(-5)	9.4(-5)	1.3(-4)
		24	0.05	7.6(-8)	1.4(-7)	2.1(-7)	2.7(-7)
	RLK	6	0.5	1.5(-3)	3.3(-3)	5.2(-3)	7.0(-3)
		12	0.2	3.1(-5)	7.1(-5)	1.1(-4)	1.5(-4)
		24	0.05	2.0(-7)	4.9(-7)	7.8(-7)	1.1(-6)
36	FD	—	0.2	2.2(-1)	5.6(-1)	9.1(-1)	1.2(+0)
	RSK	12	0.2	4.8(-5)	1.2(-4)	2.0(-4)	2.6(-4)
		24	0.05	2.1(-7)	5.2(-7)	8.2(-7)	1.1(-6)
		36	0.001	3.0(-13)	3.5(-14)	3.3(-12)	4.1(-12)
	RLK	12	0.2	4.7(-5)	1.2(-4)	1.9(-4)	2.5(-4)
		24	0.05	2.1(-7)	5.2(-7)	8.2(-7)	1.1(-6)
		36	0.001	3.0(-13)	2.7(-14)	3.3(-12)	4.1(-12)

where $W(\mathbf{r},t)$ can be either the electric field or the magnetic field. To illustrate the potential of the wavelet algorithm for electromagnetic wave simulations, we consider an analytically solvable problem

$$W(x,y,z,t) = \sin\left[\alpha_x x + \alpha_y y + \alpha_z z + \sqrt{\alpha_x^2+\alpha_y^2+\alpha_z^2/(\epsilon\mu)}t\right]$$

with periodic boundary condition. To further simplify notations, we set $\alpha_x = \alpha_y = \alpha_z = \epsilon\mu = 1$ and focus only on a cubic domain of size $(10\pi)^3$.

Two wavelet schemes: the RSK and RLK, and the FD method are considered for this problem. To test the accuracy and rate of convergence of the wavelet schemes, a variety of grid points N ($N = N_x = N_y = N_z$) and computational bandwidth M ($M = M_x = M_y = M_z$) are employed. When M =36, 24, 12, and 6, the values of r are 4.2, 3.2, 2.65 and 2.0 for the RSK and 2.95 2.75, 2.3 and 1.85 for the RLK. The fourth order Runge-Kutta scheme is used in all schemes for time discretization. Sufficiently small time increments (Δt) are used so that the major errors are due to the spatial discretization. The L_∞ errors at a number of time units are listed in TABLE 2. When $N = 24$, the number of PPW is 4.8 in each dimension. This is a typical case of under sampling and it is very difficult to achieve high computational accuracy by any means. Since usually the Yee algorithm uses about 18 PPW [4], the FD results are incorrect when $N = 24$. However, errors in the wavelet results for this difficult problem are all smaller than 0.5%. Moreover, the wavelet accuracy significantly improves as the M value is increased from 6 to 12 and 24. The last case, $M = N = 24$, corresponds to a global collocation method and its results are significantly better. In the case of $N = 36$, it is on an average about 7.2 PPW in each dimension. The accuracy of the FD method is still unsatisfactory, whereas the wavelet solutions are more accurate than those of $N = 24$. Similarly, the accuracy of the wavelet results dramatically increases as M increases. Furthermore, it is interesting to note that the wavelet algorithm attains extremely high accuracy at the global limit of $M = N = 36$.

4 Conclusion

In conclusion, this paper introduces a wavelet-collocation scheme based on the discrete singular convolution (DSC) algorithm for computational electromagnetics (CEM). The computational philosophy of the DSC-wavelet algorithm is studied. Three typical wavelet kernels are utilized to illustrate the usefulness of the proposed algorithm. The potential of the wavelet algorithm for CEM is explored by studying problems of waveguide eigenmode analysis, wave scattering simulation, electrostatics analysis, and electromagnetic wave propagations. The standard central finite difference (FD) scheme is also employed for a comparison.

It is found that the wavelet errors are usually smaller than those of the FD method by several or over ten orders of magnitude. Especially, the wavelet accuracy is found to be superior for numerically challenging problems of under sampling. The wavelet algorithm is applied to handle complex geometries, such as a T-shape waveguide and a non-uniform electrostatics domain with charge density. The non-reflecting boundary condition raised in wave scattering has also been successfully treated in the wavelet algorithm. In summary, present work indicates that the wavelet algorithm is a promising and potential approach for computational electromagnetics.

References

[1] N. Ida, *Numerical Modeling for Electromagnetic Non-destructive Evaluation*, (Chapman & Hall, London, 1995).

[2] A. Taflove and S.C. Hagness, *Computational electrodynamics: The finite-difference time-domain method*. 2nd, ed. (Artech House, Boston London, 2000).

[3] T.A. Driscoll and B. Fornberg, "A block pseudospectral method for Maxwell's equations: I. One-dimensional case," *J. Comput. Phys.*, vol. 140, pp. 47-65 (1998).

[4] D.W. Zingg, "Comparison of high-accuracy finite difference methods for linear wave propagation, " *SIAM J. Sci. Comput.*, vol. 22, pp. 476-502 (2000).

[5] I. Harari and T.J.R. Hughes, "Finite element methods for the Helmholtz equation in an exterior domain: model problems," *Comput. Meth. Appl. Mech. Eng.*, vol. 87, pp. 59-96 (1991).

[6] E. Giladi and J. B. Keller, "A hybrid numerical asymptotic method for scattering problems," *J. Comput. Phys.*, vol. 174, pp. 226-247 (2001).

[7] Z. Baharav, Y. Leviatan, "Wavelets in electromagnetics: The impedance matrix compression (IMC) method," *Int. J. Numer. Model. El.*, vol. 11(1), pp. 69-84 (1998).

[8] G. F. Wang, "A Hybrid wavelet expansion and Boundary-element analysis of electromagnetic scattering from conducting objects," *IEEE Trans. Antenn. Propag.*, vol. 43(2), pp. 170-178 (1995).

[9] G. W. Wei, "Discrete singular convolution for the solution of the Fokker-Planck equations," *J. Chem. Phys.*, vol. 110, pp. 8930–8942 (1999).

[10] G. W. Wei, "Quasi wavelets and quasi interpolating wavelets," *Chem. Phys. Lett.*, vol. 296, pp. 215-222 (1998).

[11] G.W. Wei, "Wavelet generated by using discrete singular convolution kernels," *J. Phys. A, Mathematics and General*, vol. 33, pp. 8577-8596 (2000).

[12] G.W. Wei, Y.B. Zhao and Y. Xiang, "Discrete singular convolution and its application to the analysis of plates with internal supports. I Theory and algorithm," *Int. J. Numer. Methods Engng.* vol. 55 pp. 913-946 (2002).

